Computer Simulation Results for PCM/PM/NRZ Receivers in Nonideal Channels

A. Anabtawi, T. M. Nguyen, and S. Million
Communications Systems Research Section

This article studies, by computer simulations, the performance of deep-space telemetry signals that employ the pulse code modulation/phase modulation (PCM/PM) technique, using nonreturn-to-zero data, under the separate and combined effects of unbalanced data, data asymmetry, and a band-limited channel. The study is based on measuring the symbol error rate performance and comparing the results to the theoretical results presented in previous articles. Only the effects of imperfect carrier tracking due to an imperfect data stream are considered. The presence of an imperfect data stream (unbalanced and/or asymmetric) produces undesirable spectral components at the carrier frequency, creating an imperfect carrier reference that will degrade the performance of the telemetry system. Further disturbance to the carrier reference is caused by the intersymbol interference created by the band-limited channel.

I. Introduction

There is considerable interest among international space agencies in searching for a bandwidth-efficient modulation scheme that can be used for future space missions without major modifications to their ground stations [1–4]. The Consultative Committee for Space Data Systems (CCSDS) has undertaken the task of investigating a modulation scheme that offers both of these features (bandwidth efficiency and no major hardware modifications to the current systems).

Currently, the space telemetry systems employ residual carrier modulation with subcarriers that are used to separate the data from the RF residual carrier. This was necessary to avoid interference because most of the data power fell within the bandwidth of the carrier phase-locked loop (PLL), as shown in Fig. 1(a). The CCSDS has recommended that square-wave and sine-wave subcarriers be used for the deep-space and near-Earth missions, respectively [5]. This modulation scheme is called pulse code modulation/phase-shift keying/phase modulation (PCM/PSK/PM), and it was developed at a time when weak signals and low data rates dominated [6]. With the development of technology and the evolvement of the Deep Space Network (DSN), a significant increase in the signal power can result in higher data rates. Using subcarriers in this case causes the occupied bandwidth to increase significantly. This is prohibitive because the space telemetry systems often operate under imposed bandwidth constraints. A natural solution is to eliminate the subcarrier and modulate the nonreturn-to-zero (NRZ) data directly on the RF carrier. This modulation scheme is referred to as PCM/PM/NRZ, and not only does it require
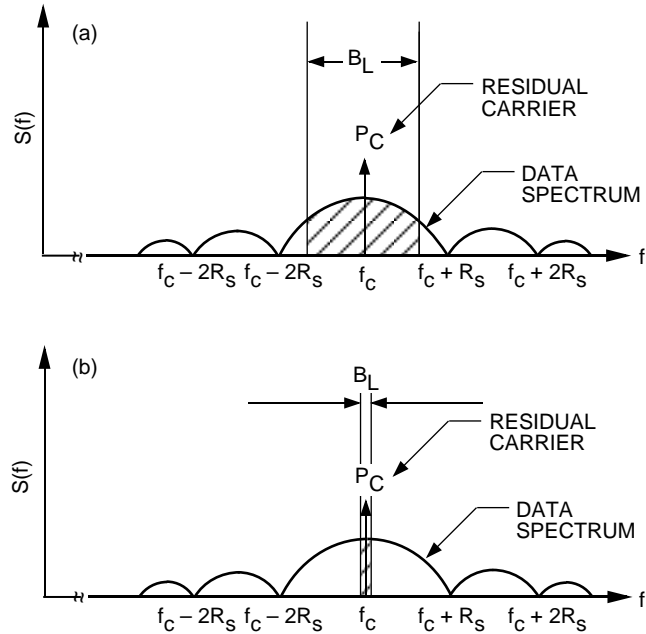
Fig. 1. PCM/PM/NRZ modulation: (a) low data rate: high ratio of loop bandwidth to data rate and (b) high data rate: low ratio of loop bandwidth to data rate.

minimum hardware modifications to the current systems, but it also achieves the bandwidth efficiency [4,7]. In this modulation technique, the part of the data spectrum that falls within the narrow carrier loop bandwidth seems flat and appears as white noise, as shown in Fig. 1(b), and, since the ratio of loop bandwidth to data rate is very small, the carrier tracking performance degradation due to this white noise component is negligible.

Recently, Nguyen has investigated and analyzed the behavior of PCM/PM receivers in nonideal channels [1,2]. The imbalance between +1's and −1's and/or data asymmetry in the data stream produce undesirable spectral components that degrade the performance of the system. Further degradation is caused by the intersymbol interference (ISI) created by the band-limited channel. This article verifies, by computer simulations, the theoretical results presented in [1,2] for the NRZ data stream. The Signal Processing Worksystem (SPW) was used for implementing and simulating the system. The separate effects of unbalanced data, data asymmetry, and band-limited channel on the symbol error rate (SER) performance of PCM/PM/NRZ receivers were simulated and then compared to the theoretical results presented in [1]. In reality, however, the receivers operate in the aggregate presence of these three effects, and the symbol signal-to-noise ratio (SSNR) degradation due to the three effects is not the algebraic sum of the SSNR degradation due to each separate effect. The second part of this article presents the simulation results for the degradation due to the combined effects on the SER performance, and these results are compared to the theoretical results presented in [2].

The organization of this article is as follows: Section II describes the separate effects on PCM/PM/NRZ receivers of perfect, unbalanced, asymmetric, and band-limited data streams. Section III describes the combined effects of these streams on PCM/PM/NRZ receivers. Section IV gives a brief description of the PCM/PM receiver blocks that were used to build the system in the SPW, Section V discusses the simulation results and compares them to theory, and, finally, Section VI presents the conclusion.

II. Separate Effects on PCM/PM/NRZ Receivers

The deep-space received telemetry signal, in the absence of a subcarrier, is given by [1]

$$s_r(t) = \sqrt{2P} \left\{ \cos\left(m_T\right) \cos\left(\omega_c t + \theta_0\right) - d(t) \sin\left(m_T\right) \sin\left(\omega_c t + \theta_0\right) \right\} + n(t) \tag{1}$$

where P is the transmitted power, m_T is the telemetry modulation index in rad, $\omega_c = 2\pi f_c$ is the angular carrier center frequency in rad/s, θ_0 is the initial carrier phase, $n(t)$ is an additive white Gaussian noise (AWGN), and $d(t)$ is the data stream (NRZ) defined as

$$d(t) = \sum_{k=-\infty}^{\infty} d_k p(t + kT_s) \tag{2}$$

where $d_k = \pm 1$ with transition density p_t, $p(t)$ is the baseband pulse, and T_s is the symbol period in seconds. The first and second terms of Eq. (1) are the residual carrier and data components, respectively.

The undesired spectral components caused by the imperfect data stream (unbalanced data and/or data asymmetry) can degrade the carrier tracking performance. If $\hat{\theta}$ denotes the carrier loop estimate of θ_0, the phase error due to the thermal noise and interference caused by the imperfect data stream is defined as

$$\theta_e = \theta_0 - \hat{\theta} = \theta_e(noise) + \theta_e(data) + \theta_e(spike) \tag{3}$$

where $\theta_e(noise)$, $\theta_e(data)$, and $\theta_e(spike)$ are the phase error caused by the noise, data interference, and the spike caused by the imperfect data stream, respectively.

The carrier loop tracks the residual carrier component in Eq. (1) to provide an imperfect reference given by

$$r(t) = \sqrt{2} \cos\left(\omega_c t + \hat{\theta}\right) \tag{4}$$

The average probability of error due to the imperfect carrier tracking is given by

$$P_e = \int_{\theta_e} P_e(\theta_e) P(\theta_e) \, d\theta_e \tag{5}$$

where $P_e(\theta_e)$ is the conditional probability of error, and $P(\theta_e)$ is the probability density function (pdf) of the carrier tracking phase error θ_e. Assuming that this pdf has a Tikhonov distribution that is entirely characterized by the mean (assumed 0) and variance σ^2 of θ_e, and when the loop signal-to-noise ratio (SNR) is high, $P(\theta_e)$ may be approximated as Gaussian distribution, namely,

$$P(\theta_e) \approx \frac{\exp\left(-\theta_e^2/(2\sigma^2)\right)}{[2\pi\sigma^2]^{-1/2}}, -\infty < \theta_e < \infty \tag{6}$$

As mentioned above, this expression was derived assuming the mean of the phase error θ_e to be zero. This assumption, however, is not true for an imperfect data stream, as will be shown in the subsequent sections.

The expressions for $P_e(\theta_e)$ and the carrier tracking phase error variance σ^2 have been evaluated in [1,2] for all the different cases studied in this article. The final results will be presented here for completeness.

A. Perfect Data Stream

In a perfect purely random data stream, the probability of transmitting a $+1$ pulse (or probability of mark), p, is equal to the probability of transmitting a -1, q, with transition density, p_t, given by

$$p_t = 2pq = \frac{1}{2} \tag{7}$$

where $q = 1 - p$.

The carrier term of Eq. (1) generates a residual carrier at f_c with power, P_c, given by

$$P_c = P \cos^2(m_T) \tag{8}$$

Combining the carrier and data terms, the one-sided power spectrum of a PCM/PM/NRZ perfect data stream is given by

$$S(f) = S_c(f) + S_D(f) \tag{9}$$

where

$$S_c(f) = P_c \delta(f) \tag{10}$$

and

$$S_D(f) = P \sin^2(m_T) S_{cont}(f) \tag{11}$$

is the data spectrum with power P_D defined as

$$P_D = P \sin^2(m_T) \tag{12}$$

For a perfect NRZ data stream, $S_{cont}(f)$ is defined as the power spectral density (PSD) for an ideal NRZ data stream and is given by

$$S_{cont}(f) = T_s \left\{ \frac{\sin^2(\pi f T_s)}{(\pi f T_s)^2} \right\} \tag{13}$$

Figure 2(a) shows the power spectrum of a perfect NRZ data stream (generated using SPW for symbol rate $R_s = 1/T_s = 10^4$ kbits/s).

For a perfect data stream and ideal channel, the conditional probability of error is given by

$$P_e(\theta_e) = \frac{1}{2} \, \text{erfc} \left\{ \sqrt{\frac{E_s}{N_0}} \cos(\theta_e) \right\} \tag{14}$$
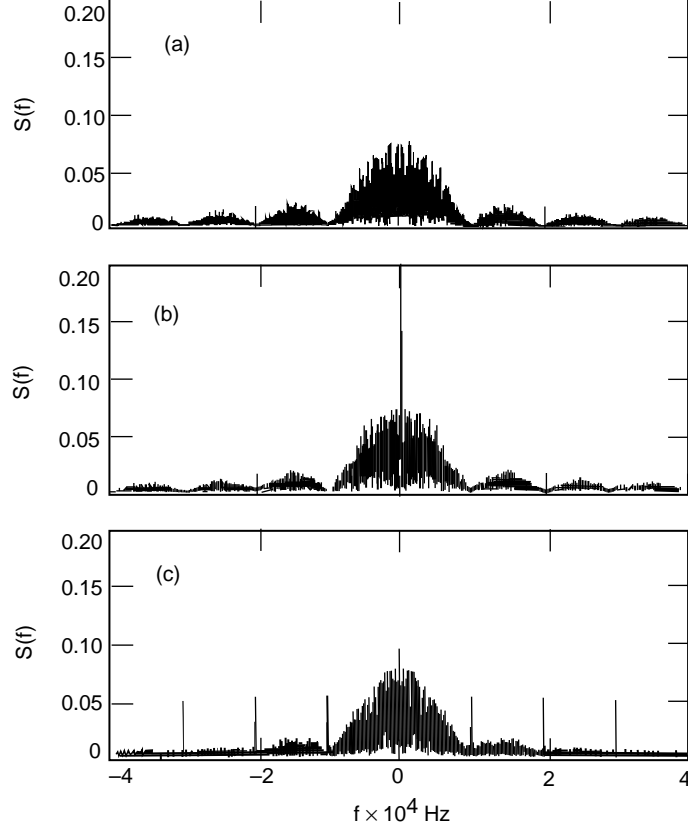
where E_s/N_0 denotes the SSNR, that is,

Fig. 2. Spectrums of different NRZ data streams: (a) balanced data stream (p = 0.5), (b) unbalanced data stream (p = 0.4), and (c) asymmetric data stream (ξ = 14 percent).

$$\frac{E_s}{N_0} = \frac{PT_s \sin^2(m_T)}{N_0} = \frac{P_D T_s}{N_0} \tag{15}$$

and erfc (x) is defined as the complementary error function given by

$$\text{erfc}(x) = 1 - \text{erf}(x) = 1 - \frac{2}{\sqrt{\pi}} \int_0^x \exp(-v^2)\,dv \tag{16}$$

Note that for this case, the mean of the phase error θ_e in the steady state is zero. This, however, is not true for an imperfect data stream, as will be shown in the subsequent sections.

For the high data rate case ($B_L/R_s \ll 0.1$, where B_L denotes the one-sided loop bandwidth), the variance of the carrier tracking phase error is given as [1]

$$\sigma^2 = \frac{1}{\rho_0} + \frac{B_L}{R_s} \tan^2(m_T) \tag{17}$$

where

$$\rho_0 = \frac{(E_s/N_0)}{(B_L/R_s)\tan^2(m_T)} \tag{18}$$

By substituting Eqs. (6) and (14) into Eq. (5) and performing the numerical integration, the curve for the probability of error versus SSNR was obtained and is shown in Figs. 3 through 9 for comparison purposes.
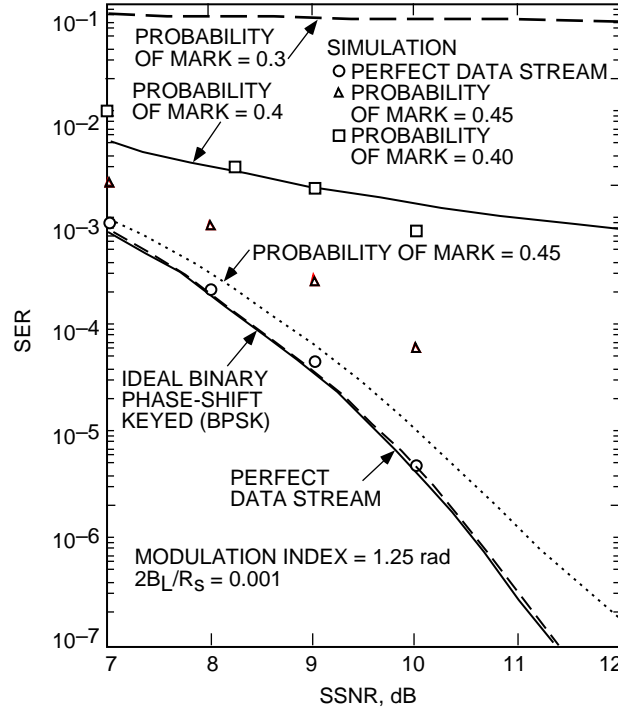

Fig. 3. Theory and simulation versus SSNR for unbalanced data without modification to the phase error.

B. Unbalanced Data Stream

The imbalance between +1's and −1's in the data stream causes an additional corruption to the received signal in Eq. (1), generating undesirable spectral components that can potentially degrade the performance of the telemetry system. When p is not equal to 0.5 (and, therefore, $p_t < 0.5$), the data component will be affected and Eq. (11) now becomes

$$S_D(f) = P\sin^2(m_T)\{S_{dc}(f) + S_{cont}(f)\} \tag{19}$$

where $S_{dc}(f)$ is the dc (or harmonic) component caused by the imperfect data stream that falls on the RF carrier.

The spectrum of an unbalanced NRZ data stream for $p = 0.4$, generated using the SPW, is shown in Fig. 2(b). For a PCM/PM/NRZ unbalanced data stream, the dc and continuous PSD components are found to be [1]
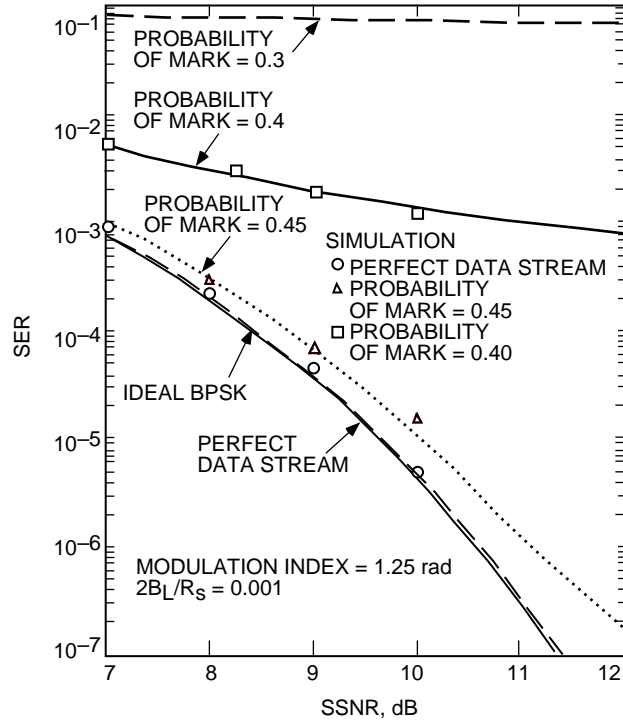
**Fig. 4. Theory and simulation SER versus SSNR
for unbalanced data.**

**Fig. 5. Theory and simulation versus SSNR for data
asymmetry.**

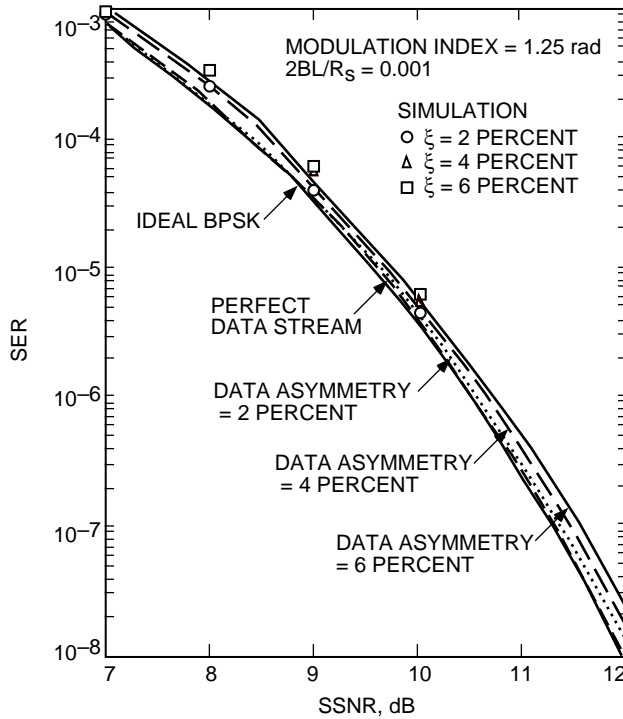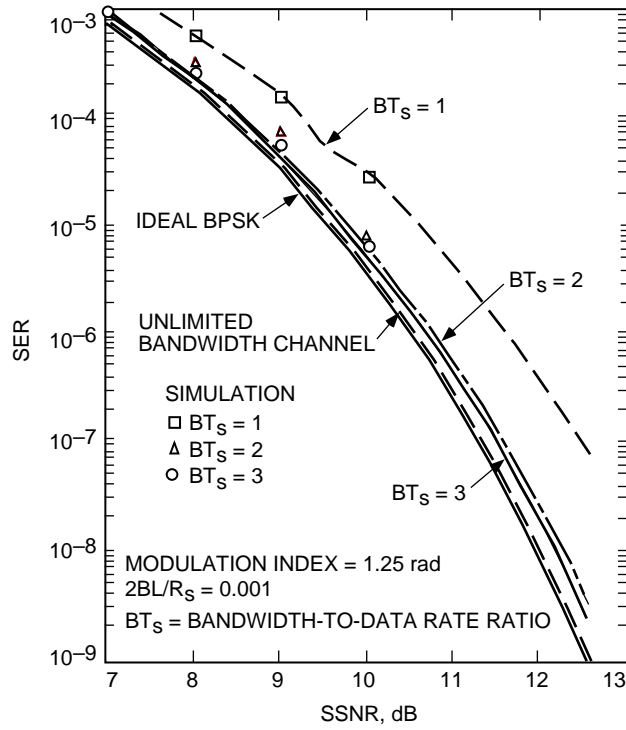**Fig. 6. Theory and simulation SER versus SSNR for band-limited channel.**
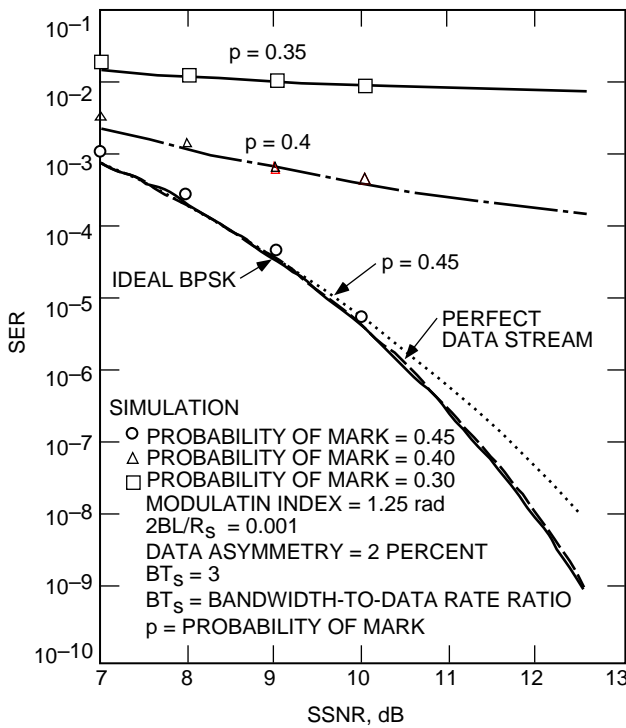

Fig. 7. Theory and simulation SER versus SSNR for various values of unbalanced data.
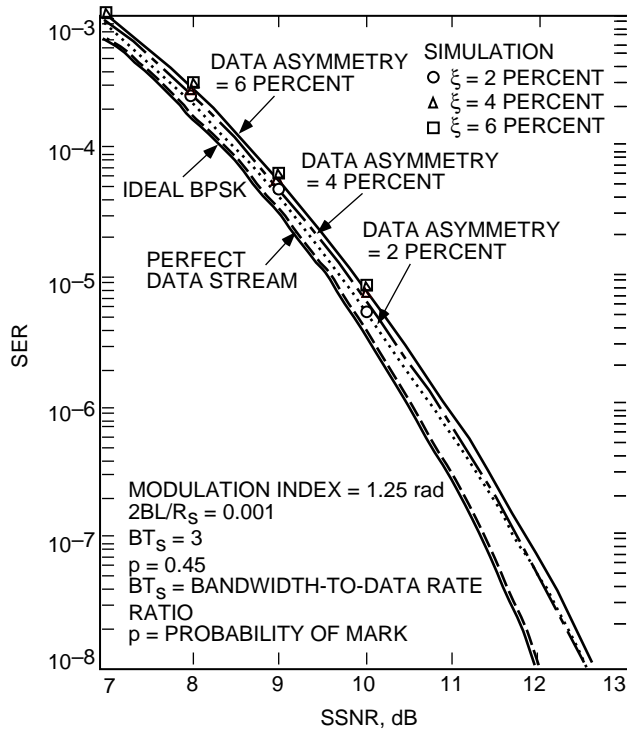
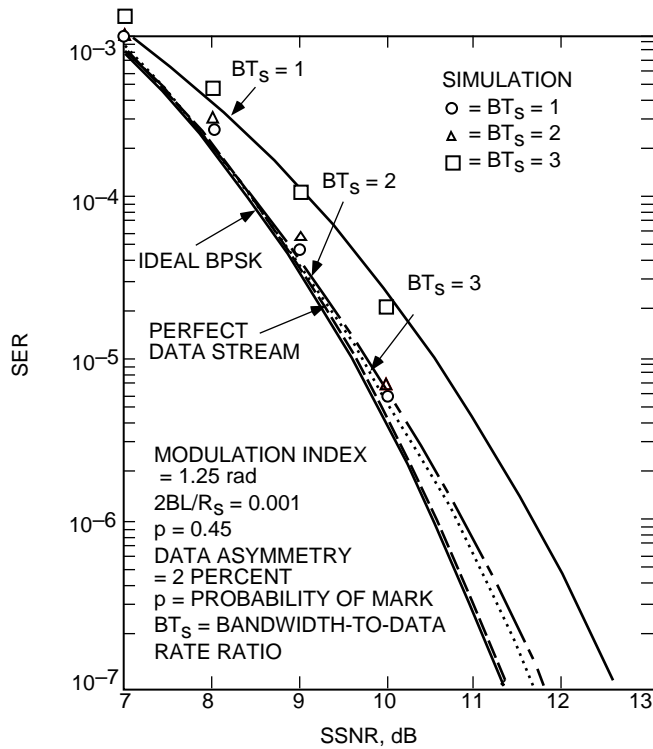**Fig. 8. Theory and simulation SER versus SSNR for various values of data asymmetry.**

Fig. 9. Theory and simulation SER versus SSNR for various values of band-limited channel.

$$S_{dc}(f) = (1 - 2p)^2 \delta(f) \tag{20}$$

$$S_{cont}(f) = 4T_s pq \left\{ \frac{\sin^2(\pi f T_s)}{(\pi f T_s)^2} \right\} \tag{21}$$

with power given by

$$P_{dc} = (1 - 2p)^2 P \sin^2(m_T) \tag{22}$$

$$P_{cont} = 4pqP \sin^2(m_T) \tag{23}$$

respectively, and where

$$P_D = P_{dc} + P_{cont} \tag{24}$$

Therefore, in addition to the tone generated at f_c by the residual carrier component in Eq. (1) with power given by Eq. (8), the spectrum of unbalanced PCM/PM/NRZ will include another tone at f_c generated by the imbalance between +1's and −1's with power given by Eq. (22). However, these two tones at f_c have noncoherent phases, causing the mean of the carrier tracking phase error in the steady state to deviate away from zero. This deviation is defined as $\theta_e(mean)$, which is a function of p and the modulation index m_T and is given by

$$\theta_e(mean) = -\tan^{-1}\{(\tan m_T)(2p - 1)\} \tag{25}$$

Note that when $p = 0.5$, then $\tan^{-1} 0 = 0$, independent of m_T, as one would expect.

Figure 10 shows the $\theta_e(mean)$ of balanced and unbalanced data streams as generated by an SPW for $\theta_0 = 0$. Note that for the case of a balanced data stream, the mean of the phase error is centered at zero, whereas for an unbalanced data stream, the mean is at a negative value which, using the above equation, is calculated to be about −0.54 rad (−31 deg) for $p = 0.6$ and $m_T = 1.25$.

The conditional probability of error $P_e(\theta_e)$ is the same as the one given by Eq. (14). Recall, however, that Eq. (6) for the pdf of the carrier tracking phase error $P(\theta_e)$ was derived assuming the mean of θ_e to be zero. Therefore, the simulations will have to compensate for the phase difference $(\theta_0 - \hat{\theta})$ (Eq. (3)) by adding the value of $\theta_e(mean)$ (Eq. (25)) to the phase of Eq. (4), ($\hat{\theta}$), which results in a zero-mean phase error. In that case, $P(\theta_e)$ is given by Eq. (6) with the tracking variance given by

$$\sigma^2 = \frac{1}{\rho_0} + \frac{\alpha}{2} \tan^2(m_T) + \frac{1}{2} \frac{I}{C} \tag{26}$$

where ρ_0 is defined as before, α is the interference due to the continuous spectrum, and I/C is the interference caused by the dc component-to-carrier power ratio given, respectively, by

$$\alpha = 4T_s p(1 - p) \int_{-\infty}^{\infty} |H(2\pi f)|^2 \frac{\sin^2(\pi f T_s)}{(\pi f T_s)^2} \, df \tag{27}$$
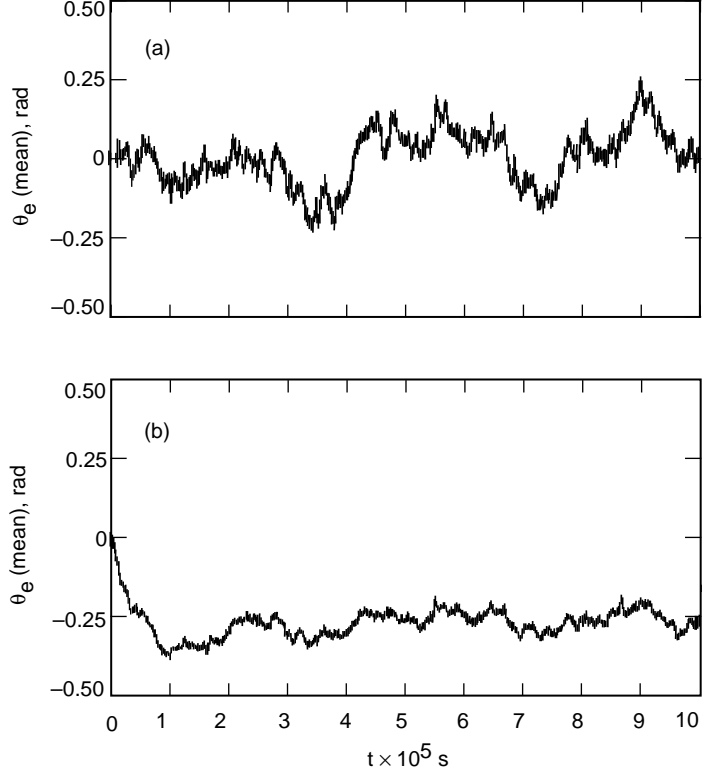
Fig. 10. θe (mean) of balanced and unbalanced data streams: (a) balanced data stream (p = 0.5): mean of phase error is centered at zero and (b) unbalanced data stream (p = 0.6): mean of the phase error deviates away from zero.

$$\frac{I}{C} = (1 - 2p)^2 \tan^2 (m_T) \tag{28}$$

where $H(j2\pi f)$ denotes the carrier loop transfer function, and for a second-order PLL is given by

$$|H(j2\pi f)|^2 = \frac{1 + 2\,(f/f_n)}{1 + (f/f_n)} \tag{29}$$

where f_n is the loop natural frequency.

The plot of the SER versus SSNR is shown in Figs. 3 and 4.

C. Data Asymmetry

Data asymmetry, due to rising and falling voltage transitions, causes undesirable spectral components that degrade the performance of the space telemetry system. The data asymmetry model adopted in this article assumes that $+1$ symbols are elongated by $(\Delta T_s)/2$ (relative to their nominal value of T_s seconds) when a negative-going data transition occurs, and -1 symbols are shortened by the same amount when a positive-going data transition occurs. Otherwise (when no transitions occur), the symbols maintain their nominal T_s seconds width. This model is illustrated in Fig. 11 for a purely random NRZ data stream.

37
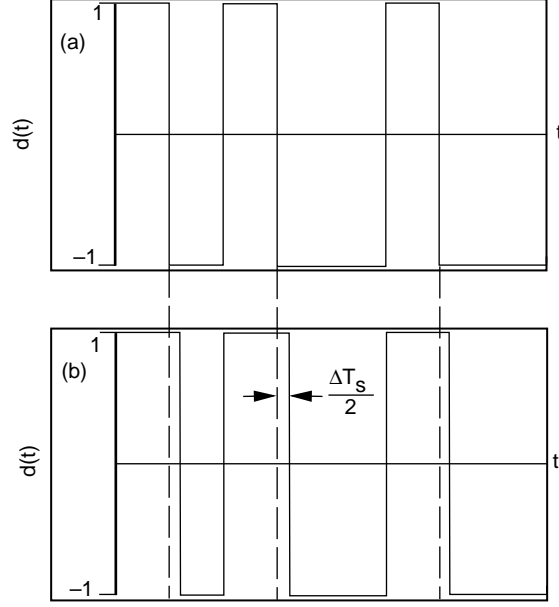
Fig. 11. Perfect and asymmetric NRZ data streams: (a) $\xi = 0$ (perfect data stream) and (b) $\xi = 0$ (asymmetric data stream).

The power spectrum of an asymmetric NRZ random data stream with equiprobable symbols (that is, $p = p_t = 0.5$) and symbol rate R_s of 10^4 kbits/s is shown in Fig. 2(c). The dc, continuous, and harmonics PSD components are given by [1,3]

$$S_{dc}(f) = \frac{1}{4}\xi^2\delta(f) \tag{30}$$

$$S_{cont}(f) \;=\; \frac{T_s}{8}\left[\frac{\sin^2(\pi f T_s)}{(\pi f T_s)^2}\right][3 + 5\,\cos^2(\pi f T_s \xi)] + \frac{T_s}{8}\left[\frac{\sin^2(2\pi f T_s \xi)}{(\pi f T_s)^2}\right][3\,\cos^2(\pi f T_s) + \cos^2(2\pi f T_s \xi)] \tag{31}$$

$$S_h(f) = \frac{1}{2\pi^2}\sum_{m=1}^{\infty}\frac{1}{m^2}C(m,\tfrac{1}{2},\xi)\delta(f - mR_s) \tag{32}$$

respectively, where ξ denotes data asymmetry and is defined as

$$\xi = \frac{\Delta}{2} \tag{33}$$

and where

$$C\left(m,\frac{1}{2},\xi\right) = \frac{1}{4}\sin^2(2m\pi\xi) \tag{34}$$

Hence, the data spectrum can be written as

38

$$S_D(f) = P \sin^2(m_T) \{S_{dc}(f) + S_{cont}(f) + S_h(f)\} \tag{35}$$

which, in addition to the tone at f_c caused by the carrier component, generates a spike at f_c due to the dc component $S_{dc}(f)$, and a spike at integer multiples of the symbol rate R_s due to the harmonics component $S_h(f)$. The continuous spectrum $S_{cont}(f)$ is plotted in Fig. 12 for various values of ξ. Note that when $\xi = 0$, the above equation reduces to the perfect NRZ random data case given by Eq. (11).

Similar to the unbalanced data case, the phase of the dc component at f_c caused by asymmetry and the phase of the carrier tone are noncoherent. The mean of the phase error θ_e for a perfectly balanced asymmetric data stream was derived to be

$$\theta_e(mean) = -\tan^{-1}\left\{(\tan m_T)\left(\frac{\xi}{2}\right)\right\} \tag{36}$$

Note that when $\xi = 0$, $\theta_e(mean) = 0$, as expected. Again, the simulations may have to compensate for the phase difference (Eq. (3)) to make the mean of θ_e zero at steady state.

Recall that in order to calculate the average probability of error, the conditional probability of error $P_e(\theta_e)$ and the tracking variance σ^2 must be determined. For the data asymmetry model used in this article and for a purely random and equiprobable (perfectly balanced) NRZ data stream, the conditional probability of error has the following form:

$$P_e(\theta_e) = \frac{5}{16}\operatorname{erfc}\left\{\sqrt{\frac{E_s}{N_0}}\cos(\theta_e)\right\} + \frac{1}{8}\operatorname{erfc}\left\{\sqrt{\frac{E_s}{N_0}}(1-\xi)\cos(\theta_e)\right\} + \frac{1}{16}\operatorname{erfc}\left\{\sqrt{\frac{E_s}{N_0}}(1-2\xi)\cos(\theta_e)\right\} \tag{37}$$

and the variance of the tracking phase error σ^2 is given by Eq. (26), where ρ_0 is defined in Eq. (18) with

$$\alpha = \int_{-\infty}^{\infty} |H(2\pi f)|^2 S_{cont}(f)\, df \tag{38}$$

and

$$\frac{I}{C} = \frac{1}{4}\xi^2 \tan^2(m_T) \tag{39}$$

Figure 5 shows the curves for SER versus SSNR when data asymmetry is present.

D. Band-Limited Channel

An additional impairment that contributes to the degradation of the overall performance of the system is the ISI caused by the band-limited channel. Band limiting causes interference between successive pulses producing the ISI effect, which behaves like an additional random noise.

If $p(t)$ denotes the pulse shape of the data, and $h'(t)$ denotes the impulse response of the equivalent low-pass filter of the RF band-pass filter with bandwidth B, then the received data can be expressed as
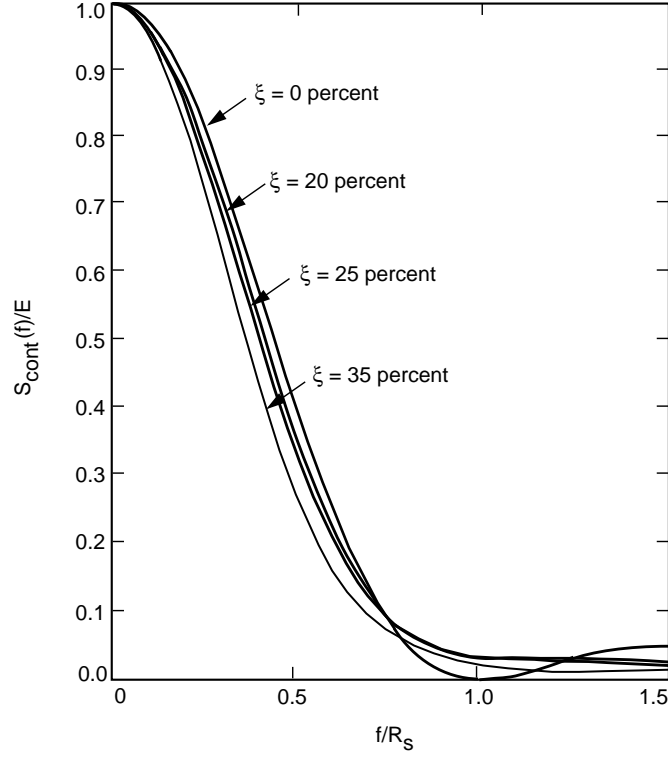
**Fig. 12. Normalized power spectrum for various values
of data asymmetry.**

$$d(t) = \sum_{k=-\infty}^{\infty} d_k g(t + kT_s) \tag{40}$$

where $d_k = \pm 1$ with $p = q = 0.5$, and $g(t)$ is given by

$$g(t) = p(t) * h'(t) \tag{41}$$

where $*$ denotes convolution.

The impulse response of an ideal channel $h'(t)$ is given by the inverse Fourier transform of the transfer function $H'(f)$:

$$H'(f) = \begin{cases} 1 & -B < \mathrm{f} < B \\ 0 & \text{otherwise} \end{cases} \tag{42}$$

resulting in

$$h'(t) = 2B \frac{\sin(2\pi Bt)}{2\pi Bt} \tag{43}$$

For an ideal filter and a perfect data stream, $g(t + kT)$ can be found to be [1]

$$g(t + kT_s) = \frac{1}{\pi} \left[Si \left\{ 2\pi B \left(t + T_s \left(k + \frac{1}{2} \right) \right) \right\} - Si \left\{ 2\pi B \left(t + T_s \left(k - \frac{1}{2} \right) \right) \right\} \right] \tag{44}$$

where

$$Si(x) = \int\limits_0^x \frac{\sin(u)}{u} \, du \tag{45}$$

Figure 13 shows a plot of $g(t)$ versus the normalized time t/T_s. Note that the shape of the output is dependent on the time-bandwidth product BT_s. For $BT_s >> 1$, the degradation due to band limiting becomes negligible. As BT_s approaches 1, the rise and fall times of the output are significant when compared to the input, and the output signal is further spread in time.

To calculate the average probability of error, $P_e(\theta_e)$ and σ^2 need to be determined. Calculating $P_e(\theta_e)$ exactly is very difficult because one has to take into account all possible combinations of the digits $d_k = \pm 1$, $1 \le |k| \le \infty$. It is assumed that only a finite number of M pulses before and after d_0, $d_0 = 0$, are taken into account. That is, only the ISI effects of the M preceding and M subsequent bits are considered on the bit under detection. For $BT_s \ge 1$, the value of $1 \le M \le 2$ is sufficient. The conditional error probability may be determined using [1]

$$P_e(\theta_e) = \frac{1}{2} \frac{1}{2^{2M}} \sum_{\substack{k = 2^{2M} \\ combinations}} \mathrm{erfc} \left\{ \sqrt{\frac{E_s}{N_0} \left[1 + \sum_{k \ne 0} d_k \lambda_k \right]} \cos(\theta_e) \right\} \tag{46}$$

where the SSNR for this case is given by

$$\frac{E_s}{N_0} = \frac{P \sin^2(m_T)}{N_0} \int\limits_0^{T_s} |g(t)|^2 \, dt \tag{47}$$

and

$$\lambda_k = \frac{\int_0^{T_s} g(t) g(t + kT_s) \, dt}{\int_0^{T_s} |g(t)|^2 \, dt} \tag{48}$$

The variance of the carrier tracking phase error is given by Eq. (17). Therefore, for $1 \le M \le 2$, the average error probability can be obtained by substituting Eqs. (6) and (46) into Eq. (5) and performing the numerical integration. The results are shown in Fig. 6.

III. Combined Effects on PCM/PM/NRZ Receivers

The practical PCM/PM/NRZ receivers operate in the presence of both an imperfect data stream and a band-limited channel. This part of the article studies the combined effects of an unbalanced data stream, data asymmetry, and ISI on the SER. The total SSNR degradation of the receivers due to these three
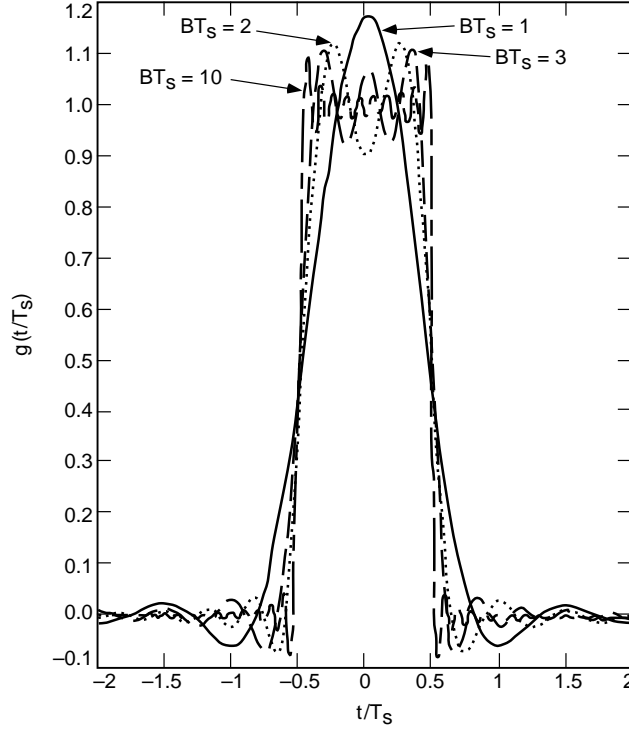
Fig. 13. Output response of the ideal filter to NRZ pulse for various values of BT_S.

undesirable effects is not the algebraic sum of the SSNR degradation due to each separate effect found in Section II. Therefore, it is necessary to study the combined effects of these three sources on the error probability performance.

For an unbalanced and asymmetric data stream, the dc, continuous, and harmonics-PSD components are given by [2]

$$S_{dc}(f) = [2p - (1 - 2\xi p_t)]^2 \delta(f) \tag{49}$$

$$S_{cont}(f) = T_s \left[\frac{\sin^2{(\pi f T_s)}}{(\pi f T_s)^2} \right] [a_1(p_t) + a_2(p, p_t, \xi)] + T_s \left[\frac{\sin^2{(\pi f T_s \xi)}}{(\pi f T_s)^2} \right] [a_3(p_t, \xi)]$$

$$+ T_s \left[\frac{\sin^2{(\pi f T_s)}}{(\pi f T_s)^2} \right] [a_4(p, p_t, \xi) - a_5(p, p_t)] \tag{50}$$

$$S_h(f) = 2 \frac{p_t^2}{\pi^2} \sum_{m=1}^{\infty} \frac{1}{m^2} C(m, p, \xi) \delta(f - mR_s) \tag{51}$$

respectively, where

$$a_1(p_t) = p_t(1 - p_t)[1 + 2(1 - p_t)] - p_t^3 \tag{52}$$

42

$$a_2(p, p_t, \xi) = \left\{ 3p_t^3 + p_t(1 - p_t)[1 + 2(1 - 2p)] \right\} \cos^2 (pfT_s\xi) \tag{53}$$

$$a_3(p_t, \xi) = p_t(1 + p_t^2 - p_t) \cos^2 (\pi fT_s) + p_t^3 \cos (2\pi fT_s\xi) \tag{54}$$

$$a_4(p, p_t, \xi) = p_t(1 - p_t)(1 - 2p)[0.5 \cos (2\pi fT_s\xi) - p \sin (2\pi fT_s\xi)] \tag{55}$$

$$a_5(p, p_t) = 0.5p_t(1 - p_t)(1 - 2p) \tag{56}$$

$$C(m, p, \xi) = \sin^2 (m\pi\xi) \left[\cos^2 (m\pi\xi) - (1 - 2p)^2 \sin^2 (m\pi\xi) \right] \tag{57}$$

Note that when $p = p_t = 1/2$ and $\xi = 0$, that is, a perfect data stream, Eqs. (49) through (51) all reduce to the result for a perfect NRZ random data stream, Eq. (13).

Once again, the presence of the two noncoherent tones (the dc component due to the imperfect data stream and the carrier tone), both at f_c, causes the mean of the phase difference $(\theta_0 - \hat{\theta})$ to deviate away from zero. The expression for the mean of this phase difference was derived to be

$$\theta_e(mean) = -\tan^{-1} \left\{ (\tan m_T)[(2p - 1) + 2\xi p(1 - p)] \right\} \tag{58}$$

Note that this equation reduces to Eq. (25) and Eq. (36) by setting $\xi = 0$ and $p = 0$, respectively.

The same approach used in Section II will be used here to determine the average SER. Therefore, the simulations will again have to compensate for the phase difference $(\theta_0 - \hat{\theta})$. The average probability of error is given by Eq. (5), and therefore, the expressions for $P_e(\theta_e)$ and $P(\theta_e)$ must be determined to evaluate P_e. The conditional error probability in the presence of an imperfect data stream and band-limited channel is given by [2]

$$P_e(\theta_e) = p \, \overline{\Pr \left\{ Z(T_s) < \frac{0}{\theta_e}, d_0 = +1 \right\}} + q \, \overline{\Pr \left\{ Z(T_s) > \frac{0}{\theta_e}, d_0 = -1 \right\}} \tag{59}$$

where the overbar denotes statistical averaging over the joint distribution of the double infinite data sequence d_k, and the test statistic $Z(T_s)$ is given by

$$Z(T_s) = E_s \left[\pm 1 + \sum_{\substack{k=-\infty \\ k \neq 0}}^{k=\infty} d_k \lambda_k(i) \right] \cos (\theta_e) + n(T_s) \tag{60}$$

where ± 1 corresponds to $d_0 = \pm 1$. It is assumed that the corrupting noise process $n(T_s)$ is a zero-mean Gaussian random variable with a variance $N_0T_s/2$. The parameter $\lambda_k(i)$ is defined as

$$\lambda_k(i) = \frac{\displaystyle\int_0^{T_s} g(t)g_i(t + kT_s) \, dt}{\displaystyle\int_0^{T_s} |g(t)|^2 \, dt}, \quad i = 1, 2, 3, 4 \tag{61}$$

where $g(t)$ is the output of the ideal filter for a perfect data stream given by Eq. (44), and $g_i(t)$ for $i = 1, 2, 3, 4$ is defined as [2]

$$g_1(t + kT_s) = \frac{1}{\pi} \left[Si \left\{ 2\pi B \left(t + T_s \left(k + \frac{1}{2} \right) \right) \right\} - Si \left\{ 2\pi B \left(t + T_s \left(k - \frac{1}{2} - \xi \right) \right) \right\} \right] \tag{62}$$

$$g_2(t + kT_s) = -\frac{1}{\pi} \left[Si \left\{ 2\pi B \left(t + T_s \left(k + \frac{1}{2} \right) \right) \right\} - Si \left\{ 2\pi B \left(t + T_s \left(k - \frac{1}{2} + \xi \right) \right) \right\} \right] \tag{63}$$

$$g_3(t + kT_s) = \frac{1}{\pi} \left[Si \left\{ 2\pi B \left(t + T_s \left(k + \frac{1}{2} \right) \right) \right\} - Si \left\{ 2\pi B \left(t + T_s \left(k - \frac{1}{2} \right) \right) \right\} \right] \tag{64}$$

$$g_4(t + kT_s) = -g_3(t + kT_s) \tag{65}$$

The variance of the carrier tracking phase error σ^2 can be obtained using Eq. (26) where

$$\alpha = \int_{-\infty}^{\infty} |H(2\pi f)|^2 S_{cont}(f) \, df \tag{66}$$

and

$$\frac{I}{C} = [2p - (1 - 2\xi p_t)]^2 \tan^2(m_T) \tag{67}$$

Again, α is the interference due to the continuous spectrum component, and I/C is the interference caused by the dc component-to-carrier power ratio. The harmonic components caused by asymmetry do not interfere with the carrier tracking because of the assumption that $2B_L << R_s$.

The average probability of error can be found by substituting Eqs. (6) and (59) into Eq. (5) and performing the numerical integration. The results are shown in Figs. 7 through 9.

IV. Description of PCM/PM Receiver Blocks

Figure 14 shows the block diagram of a PCM/PM receiver. This receiver consists of the test signal generator (TSG), the advanced receiver (ARX), and the error counter. The TSG, shown in Fig. 15, generates the deep-space spacecraft signal at an intermediate frequency (IF). The TSG's random data block controls the parameter p, and depending on this value, a balanced or unbalanced data stream is generated. The data asymmetry block controls the parameter ξ, producing an asymmetric data stream. The Appendix gives a brief description of this block. Setting $p = 0.5$ and $\xi = 0$ will produce a perfect purely random data stream. Setting $p \neq 0.5$, $\xi \neq 0$, or the combination will result in an unbalanced data stream, asymmetric data stream, or a data stream with the combined imperfections, respectively.

Fig. 14. PCM/PM/NRZ system block diagram as implemented in SPW.

Other TSG parameters include the following (the values shown are the ones used in simulations):

$$500 \times 10^3 \text{ Hz } = \text{ sampling rate, } f_s$$
$$10 \times 10^3 \text{ Hz } = \text{ symbol rate, } R_s$$
$$100 \times 10^3 \text{ Hz } = \text{ carrier frequency, } f_c$$
$$0 \deg = \text{ initial carrier phase, } \theta_0$$
$$71.62 \deg = \text{ modulation index, } m_T \text{ (corresponding to 1.25 rad)}$$

and the total power-to-noise ratio P/N_0 is calculated using

$$\frac{P}{N_0} = \frac{E_s}{N_0} - 10 \log_{10}(\sin^2 m_T) + 10 \log_{10} R_s \tag{68}$$

where E_s/N_0 is the SSNR in dB.

The ARX, shown in Fig. 16, consists of the following blocks:

45

SAMPLING RATE, f_s:	5×10^5 Hz
CARRIER FREQUENCY, f_c:	1×10^5 Hz
INITIAL CARRIER PHASE, θ_0:	0.0 deg
SYMBOL RATE, R_s:	1×10^4 Hz
MODULATION INDEX, m_T:	71.62 deg
TOTAL POWER/NOISE RATIO, P/N_0:	47.455 dB-Hz
PROBABILITY OF ZERO, p:	0.5
NO. OF SAMPLES/SYMBOL	50.0
DATA ASYMMETRY, ξ:	0.0
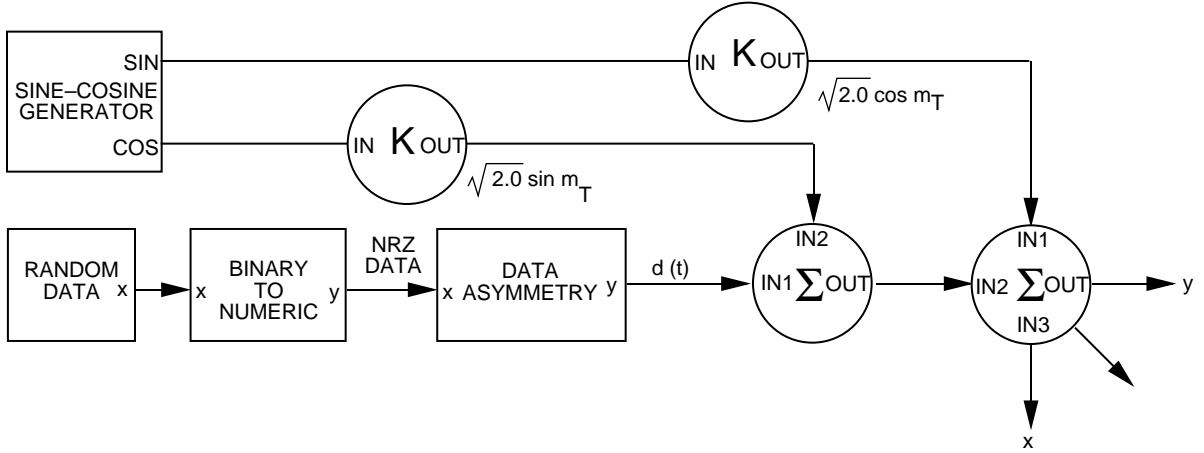
Fig. 15. Test signal generator (TSG) block diagram.

(1) The carrier PLL block estimates the incoming carrier phase and frequency and mixes it with the input signal.

(2) The phase imbalance block adds (or subtracts) a phase to its input according to the value of the phase imbalance parameter. The input to this block in simulations is given by Eq. (4); therefore, depending on the kind of imperfect data stream present, this parameter is set to $\theta_e(mean)$, as given by Eqs. (25), (36), or (58), so that by adding this phase to the incoming phase $\hat{\theta}$, the output of the block will have a zero-mean phase error. The phase imbalance parameter is set to zero when no phase compensation is required, that is, when no unbalanced and/or asymmetric data streams are present.

(3) The Butterworth low-pass filter controls the presence of the band-limiting effect by setting the filter bandwidth B to a value that depends on the product BT_s. If no band limiting is present, the filter bandwidth B is set to 100 kHz.

(4) The ideal clock generates the timing for the sum-dump-hold symbol block. The use of an ideal clock to produce the timing instead of the digital data transition tracking loop block was for the purpose of matching the assumption made in theory, and therefore, eliminating the loss due to symbol synchronization.

(5) The sum-dump-hold block outputs the soft symbols.

Finally, the error counter block compares the soft symbols of the ARX to the transmitted symbols and outputs the number of errors N.

CARRIER PARAMETERS

NUMERICALLY CONTROLLED OSCILLATOR (NCO) FREQUENCY:	1×10^5 Hz
INITIAL NCO PHASE:	0.0 deg
CARRIER UPDATE RATE:	5×10^5 Hz
ONE-SIDED LOOP BANDWIDTH, B_L, CARRIER:	5.0 Hz

INPUT PARAMETERS

SAMPLING RATE, f_S:	5×10^5 Hz
CARRIER FREQUENCY, f_C:	1×10^5 Hz
INITIAL CARRIER PHASE, θ_0:	0.0 deg
SYMBOL RATE, R_S:	1×10^4 Hz
MODULATION INDEX, m_T:	71.62 deg
TOTAL POWER/NOISE RATIO, P/N_0:	47.455 dB-Hz

CLOCK START TIME (ϕ –INTERVAL –1)	8
FILTER ORDER	3
ATTENUATION AT PASSBAND EDGE	3.0 Hz
PASSBAND EDGE FREQUENCY	3×10^4 Hz
PHASE IMBALANCE	0 .0 deg

Fig. 16. Advanced receiver block diagram.

V. Discussion and Simulation Results

By substituting the expressions for the conditional probability of error $P_e(\theta_e)$ and the probability density function for the phase error $P(\theta_e)$ into Eq. (5), the SER as a function of SSNR was plotted in [1,2] for each of the cases discussed above. Using typical operating conditions of $m_T = 1.25$ rad and $2B_L/R_S = 0.001$, these theoretical plots are shown in Figs. 3 through 9 as the continuous curves. The computer simulation results are shown as the triangular, circular, and square points for variables shown therein.

Using the SPW, simulations were performed at 7-, 8-, 9- and 10-dB SSNR (E_s/N_0), and the corresponding P/N_0 was calculated. The result of each simulation was the number of errors N (produced by the error counter as a result of comparing the soft symbols to the transmitted ones). The average error probability P_e was then calculated using

$$P_e = \frac{N}{\text{number of iterations}/(f_s/R_s)} \tag{69}$$

where f_s is the sampling frequency in Hz and the fraction (f_s/R_s) is the number of samples per symbol. The number of iterations must be chosen large enough so that the simulation results have sufficient statistics. That is,

$$\text{number of iterations} = \frac{100}{\text{SER}} \left(\frac{f_s}{R_s} \right) \tag{70}$$

where SER is the symbol error rate as given by the theory. Finally, P_e was plotted versus SSNR and the results were compared to the theoretical curves presented in [1,2].

A. Unbalanced Data

To verify the performance of the receiver in the presence of an unbalanced data stream, simulations were performed for $p = 0.5$, 0.45, and 0.4.

As mentioned in Section II.B, when $p \neq 0.5$, the phase of the tone caused by the unbalanced data is noncoherent with the carrier phase, which results in a nonzero-mean phase error θ_e. In order to overcome this problem, the phase error was calculated using Eq. (25), checked by simulations, and then modified so that the resultant phase error is of zero mean.

Figure 3 shows the theoretical and simulation results when no phase modification is made to the phase error. When $p \neq 0.5$, the simulations are in disagreement with theory, and the SSNR degradation in some cases exceeds 1 dB. On the other hand, when the phase error is modified, the theoretical and simulation results are in good agreement. These results are presented in Table 1 and Fig. 4. It is obvious that as p deviates from 0.5, the performance of PCM/PM/NRZ degrades significantly, and that the degradation becomes unacceptable when $p < 0.45$. This is due to the presence of a strong dc component caused by the unbalanced data stream at the carrier frequency. The higher the deviation from 0.5, the stronger the dc component, and as a result, the worse the degradation.

Table 1. Simulation data and results for unbalanced data, separate effects.[a]

Probability of mark	E_s/N_0, dB	P/N_0, dB	No. of iterations in millions	No. of errors	P_e	P_e theory
0.5	7	47.455	6	105	8.75×10^{-4}	7.727×10^{-4}
0.5	8	48.455	28.2	126	2.23×10^{-4}	1.909×10^{-4}
0.5	9	49.455	150	116	3.87×10^{-5}	3.363×10^{-5}
0.5	10	50.455	1300	132	5.08×10^{-6}	3.872×10^{-6}
0.45	7	47.455	6.01	115	9.57×10^{-4}	1.100×10^{-3}
0.45	8	48.455	25.2	129	2.56×10^{-4}	3.100×10^{-4}
0.45	9	49.455	80.2	112	6.98×10^{-5}	6.600×10^{-5}
0.45	10	50.455	500.2	134	1.34×10^{-5}	1.100×10^{-5}
0.4	7	47.455	7	764	5.79×10^{-3}	5.400×10^{-3}
0.4	8	48.455	10.0	704	3.52×10^{-3}	3.250×10^{-3}
0.4	9	49.455	15	612	2.04×10^{-3}	2.000×10^{-3}
0.4	10	50.455	25	686	1.37×10^{-3}	1.500×10^{-3}

[a] $m = 1.25$ rad, $R_s = 1 \times 10^4$ Hz, $f_s = 5 \times 10^5$ Hz, $B_L = 5$ Hz, $2B_L/R_s = 0.001$.

B. Data Asymmetry

Since the power of the dc component generated by the asymmetric data at f_c is much less than the power of the carrier tone, the mean of the phase error will be small. The mean was calculated (Eq. (36)) and measured to be between -1.7 and -5.2 deg for ξ between 2 and 6 percent, respectively, which are the minimum and maximum values for ξ used in the simulations. The degradation due to this nonzero-mean phase error is negligible and, hence, no compensation was done to the phase error. Simulations were performed for $\xi = 2, 4$, and 6 percent. The results are shown in Table 2 and Fig. 5. Again the simulation results are in good agreement with the theoretical results (within 0.2 dB). The numerical results show

that, for data asymmetry less than or equal to 2 percent, the SSNR degradation is on the order of 0.1 dB or less, and that this degradation is between 0.2 dB and 0.25 dB for data asymmetry of 6 percent and for $10^{-7} \leq \text{SER} \leq 10^{-5}$.

Table 2. Simulation data and results for data asymmetry, separate effects.[a]

Data asymmetry, percent	E_s/N_0, dB	P_t/N_0, dB	No. of iterations in millions	No. of errors	P_e	P_e theory
2	7	47.455	6.6	124	9.39×10^{-4}	8.75×10^{-4}
2	8	48.455	23	119	2.59×10^{-4}	2.20×10^{-4}
2	9	49.455	130	139	5.35×10^{-5}	3.85×10^{-5}
2	10	50.455	2100	203	4.83×10^{-6}	4.80×10^{-6}
4	7	47.455	6.6	144	1.09×10^{-3}	9.60×10^{-4}
4	8	48.455	20	137	3.43×10^{-4}	2.60×10^{-4}
4	9	49.455	115	136	5.91×10^{-5}	4.40×10^{-5}
4	10	50.455	1900	253	6.66×10^{-6}	5.50×10^{-6}
6	7	47.455	6.6	146	1.11×10^{-3}	1.30×10^{-3}
6	8	48.455	18	125	3.47×10^{-4}	2.85×10^{-4}
6	9	49.455	108	132	6.11×10^{-5}	4.70×10^{-5}
6	10	50.455	800	138	8.63×10^{-6}	6.30×10^{-6}

[a] $p = 0.5$, $m = 1.25$ rad, $R_s = 1 \times 10^4$ Hz, $f_s = 5 \times 10^5$ Hz, $B_L = 5$ Hz, $2B_L/R_s = 0.001$.

C. Band-Limited Channel

In order to test the effect of the band-limited channel on the overall performance of the system, simulations were performed for different values of the time-bandwidth product $BT_s = 1, 2$, and 3. As expected, the higher the value of the product BT_s, the better the performance of the system. The simulation results are shown in Table 3 and Fig. 6. The numerical results show that for $10^{-7} \leq \text{SER} \leq 10^{-5}$, the SSNR degradation is in the range of 1 to 1.2 dB for $BT_s = 1$, and less than 0.3 for $BT_s = 2$. The theoretical and simulation results are in good agreement. However, the simulations are a little worse than the theoretical results. This is because the theoretical results were obtained for the case when the ISI is caused by two adjacent pulses, that is, two pulses before and two pulses after the current pulse is considered in the SER calculation.

D. Combined Effects

To test the behavior of PCM/PM/NRZ receivers in the presence of the combination of the three undesirable effects, simulations were performed for different values of p, ξ, and BT_s. One of the parameters was varied as the other two remained constant. Since data imbalance and asymmetry were always present, all simulations required compensation for the phase error $\theta_e(mean)$ (Eq. (58)) so that the result is a zero-mean phase error.

Figure 7 plots the SER as a function of SSNR for a fixed data asymmetry ξ of 2 percent and $BT_s = 3$ with p, probability of mark, as a parameter. The simulation results are also shown in Table 4, and are in good agreement with the theory. The results indicate that, for $m_T = 1.25$ rad and $2B_L/R_S = 0.001$, the SER degrades seriously as p deviates from 0.45.

Table 3. Simulation data and results for a band-limited channel, separate effects.[a]

BT_s	E_s/N_0, dB	P/N_0, dB	No. of iterations in millions	No. of errors	P_e	P_e theory
1	7	47.455	6	226	1.88×10^{-3}	1.80×10^{-3}
1	8	48.455	11	141	6.41×10^{-4}	5.80×10^{-4}
1	9	49.455	30	94	1.57×10^{-4}	1.70×10^{-4}
1	10	50.455	160	88	2.75×10^{-5}	3.30×10^{-5}
2	7	47.455	6	150	1.25×10^{-3}	9.20×10^{-4}
2	8	48.455	21	146	3.48×10^{-4}	2.50×10^{-4}
2	9	49.455	105	143	6.81×10^{-5}	4.83×10^{-5}
2	10	50.455	800	137	8.56×10^{-6}	6.50×10^{-6}
3	7	47.455	6	125	1.04×10^{-3}	8.60×10^{-4}
3	8	48.455	22.6	131	2.90×10^{-4}	2.30×10^{-4}
3	9	49.455	114	126	5.53×10^{-5}	4.40×10^{-5}
3	10	50.455	800	124	7.75×10^{-6}	5.60×10^{-6}

[a] $m = 1.25$ rad, probability of mark $= 0.5$, $R_s = 1 \times 10^4$ Hz, $f_s = 5 \times 10^5$ Hz, $B_L = 5$ Hz, $2B_L/R_s = 0.001$.

Table 4. Simulation data and results for various probabilities of mark, combined effects.[a]

Probability of mark	E_s/N_0, dB	P/N_0, dB	No. of iterations in millions	No. of errors	P_e	P_e theory (approximate)
0.45	7	47.455	7.2	149	1.03×10^{-3}	7.80×10^{-4}
0.45	8	48.455	25.2	137	2.72×10^{-4}	2.00×10^{-4}
0.45	9	49.455	80.2	78	4.86×10^{-5}	3.60×10^{-5}
0.45	10	50.455	500.2	57	5.70×10^{-6}	5.40×10^{-6}
0.4	7	47.455	7.2	467	3.24×10^{-3}	2.20×10^{-3}
0.4	8	48.455	25.2	711	1.41×10^{-3}	1.25×10^{-3}
0.4	9	49.455	80.2	983	6.13×10^{-4}	6.50×10^{-4}
0.4	10	50.455	500.2	4.23×10^3	4.23×10^{-4}	3.85×10^{-4}
0.35	7	47.455	7.2	2.80×10^3	1.94×10^{-2}	1.50×10^{-2}
0.35	8	48.455	25.2	6.41×10^3	1.27×10^{-2}	1.25×10^{-2}
0.35	9	49.455	80.2	1.89×10^4	1.18×10^{-2}	1.00×10^{-2}
0.35	10	50.455	500.2	8.72×10^4	8.72×10^{-3}	9.00×10^{-3}

[a] Data asymmetry $= 2$ percent, $BT_s = 3$, $m = 1.25$ rad, $R_s = 1 \times 10^4$ Hz, $f_s = 5 \times 10^5$ Hz, $B_L = 5$ Hz, $2B_L/R_s = 0.001$.

Table 5 shows the simulation results obtained for various values of data asymmetry ξ with $BT_s = 3$ and $p = 0.45$. As shown in Fig. 8, the simulations are in good agreement with the theory. It is also obvious that PCM/PM/NRZ is not sensitive to data asymmetry since the SSNR degradation is between 0.1 and 0.5 dB when ξ varies between 2 and 6 percent and the SER is between 10^{-4} and 10^{-7}.

Table 5. Simulation data and results for various values of data asymmetry, combined effects.[a]

Data asymmetry, percent	E_s/N_0, dB	P/N_0, dB	No. of iterations in millions	No. of errors	P_e	P_e theory (approximate)
2	7	47.455	7.2	149	1.03×10^{-3}	7.80×10^{-4}
2	8	48.455	25.2	137	2.72×10^{-4}	2.00×10^{-4}
2	9	49.455	80.2	78	4.86×10^{-5}	3.60×10^{-5}
2	10	50.455	500.2	57	5.70×10^{-6}	5.40×10^{-6}
4	7	47.455	7.2	160	1.11×10^{-3}	9.70×10^{-4}
4	8	48.455	25.2	155	3.08×10^{-4}	2.70×10^{-4}
4	9	49.455	80.2	95	5.92×10^{-5}	4.80×10^{-5}
4	10	50.455	500.2	78	7.80×10^{-6}	6.50×10^{-6}
6	7	47.455	7.2	168	1.17×10^{-3}	1.10×10^{-3}
6	8	48.455	25.2	168	3.33×10^{-4}	2.95×10^{-4}
6	9	49.455	80.2	98	6.11×10^{-5}	5.50×10^{-5}
6	10	50.455	500.2	82	8.20×10^{-6}	7.75×10^{-6}

[a] Probability of mark = 0.45, $BT_s = 3$, $m = 1.25$ rad, $R_s = 1 \times 10^4$ Hz, $f_s = 5 \times 10^5$ Hz, $B_L = 5$ Hz, $2B_L/R_s = 0.001$.

Table 6 and Fig. 9 illustrate the SER performance in the presence of a band-limiting channel for $p = 0.45$ and $\xi = 2$ percent with BT_s as a parameter. As shown, the simulations are in good agreement with the theory, and for $BT_s = 3$, the SSNR degradation is on the order of 0.4 dB or less when the SER is between 10^{-4} and 10^{-7}.

The numerical results prove that the total SSNR degradation due to the three undesirable effects is not the algebraic sum of the SSNR degradation due to each separate effect. As an example, when the SER is 10^{-5}, the SSNR degradation when $p = 0.45$, $\xi = 2$ percent, and $BT_s = 3$ (Fig. 7) is about 0.1 dB, whereas, the algebraic sum of the SSNR degradations due to each separate effect (Figs. 4 through 6) is about 0.6 dB.

VI. Conclusion

This article studied, by computer simulations, the separate and combined effects of unbalanced data, data asymmetry, and a band-limited channel on the performance of a PCM/PM/NRZ receiver. All the simulation results were in good agreement with the theoretical results presented in [1,2]. Hence, the mathematical models presented in [1,2] can be used to predict the performance of the PCM/PM/NRZ receivers. PCM/PM/NRZ was shown to be most sensitive to the imbalance between +1's and −1's in the data stream, as the performance degradation became unacceptable when $p < 0.45$, and least sensitive to data asymmetry. For $BT_S = 3$, the SER performance was shown to be acceptable for both near-Earth and deep-space missions.

Table 6. Simulation data and results for various values of BT_s, combined effects.[a]

BT_s	E_s/N_0, dB	P/N_0, dB	No. of iterations in millions	No. of errors	P_e	P_e theory (approximate)
3	7	47.455	7.2	149	1.03×10^{-3}	7.80×10^{-4}
3	8	48.455	25.2	137	2.72×10^{-4}	2.00×10^{-4}
3	9	49.455	80.2	78	4.86×10^{-5}	3.60×10^{-5}
3	10	50.455	500.2	57	5.70×10^{-6}	5.40×10^{-6}
2	7	47.455	7.2	168	1.17×10^{-3}	8.50×10^{-4}
2	8	48.455	25.2	158	3.13×10^{-4}	2.20×10^{-4}
2	9	49.455	80.2	92	5.74×10^{-5}	3.90×10^{-5}
2	10	50.455	500.2	70	7.00×10^{-6}	6.60×10^{-6}
1	7	47.455	7.2	222	1.54×10^{-3}	1.25×10^{-3}
1	8	48.455	25.2	244	4.84×10^{-4}	3.75×10^{-4}
1	9	49.455	80.2	177	1.10×10^{-4}	1.20×10^{-4}
1	10	50.455	500.2	207	2.07×10^{-5}	2.60×10^{-5}

[a] Probability of mark = 0.45, data asymmetry = 2 percent, $m = 1.25$ rad, $R_s = 1 \times 10^4$ Hz, $f_s = 5 \times 10^6$ Hz, $B_L = 5$ Hz, $2B_L/R_s = 0.001$.

Another modulation scheme that is of interest to CCSDS is PCM/PM/Bi-ϕ, which is also known to be one of the most efficient modulation schemes in terms of bandwidth occupancy as compared to PCM/PSK/PM [4]. Mathematical models have been developed to predict the performance of PCM/PM/Bi-ϕ receivers [1,2], and these models are currently being verified by members of CCSDS and the results will be reported later.

Acknowledgments

References

[1] T. M. Nguyen, "Behavior of PCM/PM Receivers in Non-Ideal Channels, Part I: Separate Effects of Imperfect Data Streams and Bandlimiting Channels on Performances," *Report of the Proceedings of the RF and Modulation Subpanel 1E Meeting at the German Space Operations Centre, September 20–24, 1993*, CCSDS B20.0-Y-1, Consultative Committee for Space Data Systems, February 1994.

[2] T. M. Nguyen, "Behavior of PCM/PM Receivers in Non-Ideal Channels, Part II: Combined Effects of Imperfect Data Streams and Bandlimiting Channels on Performances," *Report of the Proceedings of the RF and Modulation Subpanel 1E Meeting at the German Space Operations Centre, September 20–24, 1993*, CCSDS B20.0-Y-1, Consultative Committee for Space Data Systems, February 1994.

[3] T. M. Nguyen, "The Impact of NRZ Data Asymmetry on the Performance of a Space Telemetry System," *IEEE Transactions on Electromagnetic Compatibility*, vol. 33, no. 4, November 1991.

[4] M. M. Shihabi, T. M. Nguyen, and S. M. Hinedi, "A Comparison of Telemetry Signals in the Presence and Absence of a Subcarrier," *IEEE Transactions on Electromagnetic Compatibility*, vol. 36, no. 1, February 1994.

[5] Consultative Committee for Space Data Systems, *Recommendations for Space Data System Standards, Radio Frequency and Modulation Systems, Part I, Earth Stations and Spacecraft*, CCSDS 401.0-B, Blue Book, Washington D.C.: CCSDS Secretariat, Communications and Data Systems Division (Code OS), NASA.

[6] J. Yuen, editor, *Deep Space Telecommunications Systems Engineering*, New York: Plenum Press, 1983.

[7] J. F. Pelayo and J.-L. Gerner, "PCM/PSK/PM and PCM-SPL/PM Signals—Occupied Bandwidth and Bit Error Rate," *Report of the Proceedings of the RF and Modulation Subpanel 1E Meeting at the German Space Operations Centre, September 20–24, 1993*, CCSDS B20.0-Y-1, Consultative Committee for Space Data Systems, February 1994.

Appendix

Data Asymmetry Block

The data asymmetry block outputs NRZ asymmetric data stream y when the input x is a purely random NRZ data stream. This block was implemented in SPW using mostly delays, switches, and decision blocks. It first detects the transition that occurs at the end of every symbol using

$$trans = \frac{d_k - d_{k-1}}{2} \tag{A-1}$$

where d_k is the present symbol value and d_{k-1} is the previous symbol value, and therefore, this yields a -1 when a $+1$ to -1 transition occurs, a $+1$ when a -1 to $+1$ transition occurs, and a 0 when no transition occurs. The block then determines a threshold value T_1, which is 0 if $trans = +1$ or 0, and ξ if $trans = -1$, where ξ denotes data asymmetry. If there are N samples per symbol for the input x, P denotes the past sample value, C the current, and i the ith sample in the symbol, then, for $i = 0$, $i < N$; if $i < T_1$, then $y = P$; otherwise, if $T_1 < i < N$, then $y = C$.